Bioorganic & Medicinal Chemistry 19 (2011) 1079–1084

Contents lists available at ScienceDirect

Bioorganic & Medicinal Chemistry

journal homepage: www.elsevier.com/locate/bmc

A genetically encoded sensor for H_2O_2 with expanded dynamic range

Kseniya N. Markvicheva [a], Dmitry S. Bilan [a], Natalia M. Mishina [a], Andrey Yu. Gorokhovatsky [b], Leonid M. Vinokurov [b], Sergey Lukyanov [a], Vsevolod V. Belousov [a,*]

[a] Shemyakin-Ovchinnikov Institute of Bioorganic Chemistry, RAS, Miklukho-Maklaya 16/10, 117997 Moscow, Russia
[b] Shemyakin-Ovchinnikov Institute of Bioorganic Chemistry, Pushchino Branch, RAS, Pushchino, Russia

ARTICLE INFO

Article history:
Received 19 May 2010
Revised 30 June 2010
Accepted 7 July 2010
Available online 5 August 2010

Keywords:
Hydrogen peroxide
HyPer
HyPer-2
OxyR
Imaging
GFP

ABSTRACT

Hydrogen peroxide is an important second messenger controlling intracellular signaling cascades by selective oxidation of redox active thiolates in proteins. Changes in intracellular [H_2O_2] can be tracked in real time using HyPer, a ratiometric genetically encoded fluorescent probe. Although HyPer is sensitive and selective for H_2O_2 due to the properties of its sensing domain derived from the *Escherichia coli* OxyR protein, many applications may benefit from an improvement of the indicator's dynamic range. We here report HyPer-2, a probe that fills this demand. Upon saturating [H_2O_2] exposure, HyPer-2 undergoes an up to sixfold increase of the ratio F500/F420 versus a threefold change in HyPer. HyPer-2 was generated by a single point mutation A406V from HyPer corresponding to A233V in wtOxyR. This mutation was previously shown to destabilize interface between monomers in OxyR dimers. However, in HyPer-2, the A233V mutation stabilizes the dimer and expands the dynamic range of the probe.

1. Introduction

Aerobic organisms reduce molecular oxygen to produce energy. Most of the oxygen consumed undergoes a four-electron reduction to water. However, a fraction of the oxygen within cells receives only one electron. This process gives birth to a superoxide anion radical, a highly reactive molecule serving as a precursor of other reactive oxygen species (ROS).[1,2] Under a variety of pathological conditions, ROS production in the cells increases enormously leading to oxidative stress and nonspecific oxidation of lipids, DNA, and proteins.[1] At the same time, ROS participate in normal physiology modifying cellular signaling cascades activated in response to external stimuli such as growth factors and cytokines.[3] Among ROS, H_2O_2 is best studied as a second messenger. It mainly acts in the cells by modifying critical thiol residues of proteins thereby regulating their catalytic activities or other functions. Due to the reducing conditions within the cell, H_2O_2 is able to react with only those Cys residues that have low pK_a (below 6.5) and, therefore, tend to be deprotonated at physiological pH.[2] A well-documented example of such regulation is an oxidation of protein tyrosine phosphatases (PTPs). Activation of receptor tyrosine kinases (RTKs) leads to production of H_2O_2 by NADPH oxidase (Nox) family enzymes.[4] This H_2O_2 inhibits PTPs by oxidizing their catalytic thiolates thus allowing an extended propagation of the phosphorylation cascade.[5,6]

For many decades since the discovery of biological ROS, their detection inside cells was difficult due to the absence of adequate measurement technique. Despite their high dynamic range, small molecule chemical probes for ROS detection have one or several of the following disadvantages: low specificity, poor to zero cell permeability, photodynamic ROS production leading to signal self-amplification. We overcame these drawbacks by development of the first genetically encoded sensor for H_2O_2, HyPer.[7] HyPer can be expressed in apparently any compartment of the cell by transfecting cells with DNA encoding the HyPer fusion with a subcellular localization tag or a protein of interest. HyPer has two excitation peaks corresponding to the protonated (420 nm) and charged (500 nm) forms of Tyr residue of the YFP chromophore. Both forms can be easily visualized by laser excitation of a confocal system or with widefield fluorescent microscopy. Ratiometric readout avoids artifacts associated with cell movement or differences in the sensor expression level between cells. However, for cells that do not move significantly and do not change the shape in the course of the experiment, single wavelength monitoring is possible. The properties of the H_2O_2-sensing domain of HyPer, derived from the bacterial OxyR protein,[8,9] dictate high selectivity of the probe, high sensitivity and, importantly, good reversibility in the intracellular environment.[7]

Wild-type OxyR consists of two domains, a DNA-binding and a regulatory (OxyR-RD) domain.[9] The latter contains two cysteine residues, C199 and C208, critical for the protein function as an H_2O_2 sensor. C199 resides in a hydrophobic pocket and therefore is inaccessible for charged oxidants such as superoxide anion

* Corresponding author. Tel.: +7 495 4298020; fax: +7 495 3307056.
E-mail address: vsevolod.belousov@gmail.com (V.V. Belousov).

0968-0896/$ - see front matter © 2010 Elsevier Ltd. All rights reserved.
doi:10.1016/j.bmc.2010.07.014

radical.[8] However, amphiphilic H_2O_2 molecules are able to penetrate the pocket and oxidize C199 to a sulphenic acid intermediate that is repelled by its hydrophobic surrounding due to its charge. Initially separated, C199 and C208 now get sufficiently close to form the disulphide.[10] This reaction changes the overall conformation of the OxyR-RD permitting OxyR binding to a specific region on DNA.[11] OxyR was shown to function as either dimer or tetramer (dimer of dimers)[12] and therefore contains one or two oligomerization interfaces. Crystallization of OxyR-RD reveals a dimer interface that consists of a.a. 226–233 positioned C-terminally behind the 'redox loop' that hosts C199 and C208.[8]

The dynamic range of HyPer F500/F420 ratio is 3. This is satisfactory for most of the experimental conditions. However, expansion of the dynamic range could be beneficial for applications in high-content/high-throughput imaging and imaging of low amounts of H_2O_2 produced for cell signaling. Here we report HyPer-2, the probe with the twice-expanded dynamic range compared to HyPer.

2. Results

2.1. Investigating the dynamic range of the HyPer-N353S-A406V-NES mutant

During HyPer subcloning to introduce nuclear export signal sequences (NES), we accidentally produced two random PCR-derived mutations leading to amino acid substitutions. The first mutation affected the sequence of the fluorescent protein (N353S corresponding to N121S in GFP). The other mutation was A406V corresponding to A233V in wtOxyR (Fig. 1a). When expressed in HeLa cells, this probe demonstrated expanded dynamic range compared to regular HyPer. To carefully evaluate the amplitude of the hydroperoxide response, we designed a simple assay to measure immediately [H_2O_2] changes in cells. Usually, addition of compounds to the glass-bottom cell culture dish mounted on a microscope table takes several seconds. To ensure proper mixing, the solution should be added in a large volume, not less than ¼ of the volume of the media in the dish. Adding this carefully to avoid focus shifts requires up to 10 s. Giving the large volume of the media in the dish, diffusion of the compound may also take time. In case of H_2O_2 addition imaged with HyPer, the oxidation profile may vary between dishes. We therefore used μ-slides to culture, transfect and image cells exposed to H_2O_2. The scheme of the experiment is shown in Figure 1b. The total volume of μ-slide-VI channel with its two reservoirs is 120 μl. Prior to imaging, we removed 90 μl of the medium via one of the reservoirs of the channel. The remaining 30 μl of the media were left inside the channel. We chose cells, adjusted the focus and started a time series. After acquiring the first several frames (Fig. 1c), we added 90–100 μl of H_2O_2-containing medium as a drop into the front reservoir of the channel. In this setting, the H_2O_2 medium immediately replaced the medium inside the channel.

Upon addition of saturating amounts of H_2O_2 (100 μM) to the cells expressing HyPer-N353S-A406V-NES, the F500/F420 ratio of the probe changed 6- to 7-fold (Fig. 1c and d).

2.2. HyPer-2 dynamics in living cells

The reason for the dynamic range expansion could be the NES attached to the C-terminus of HyPer, or one of two amino acid

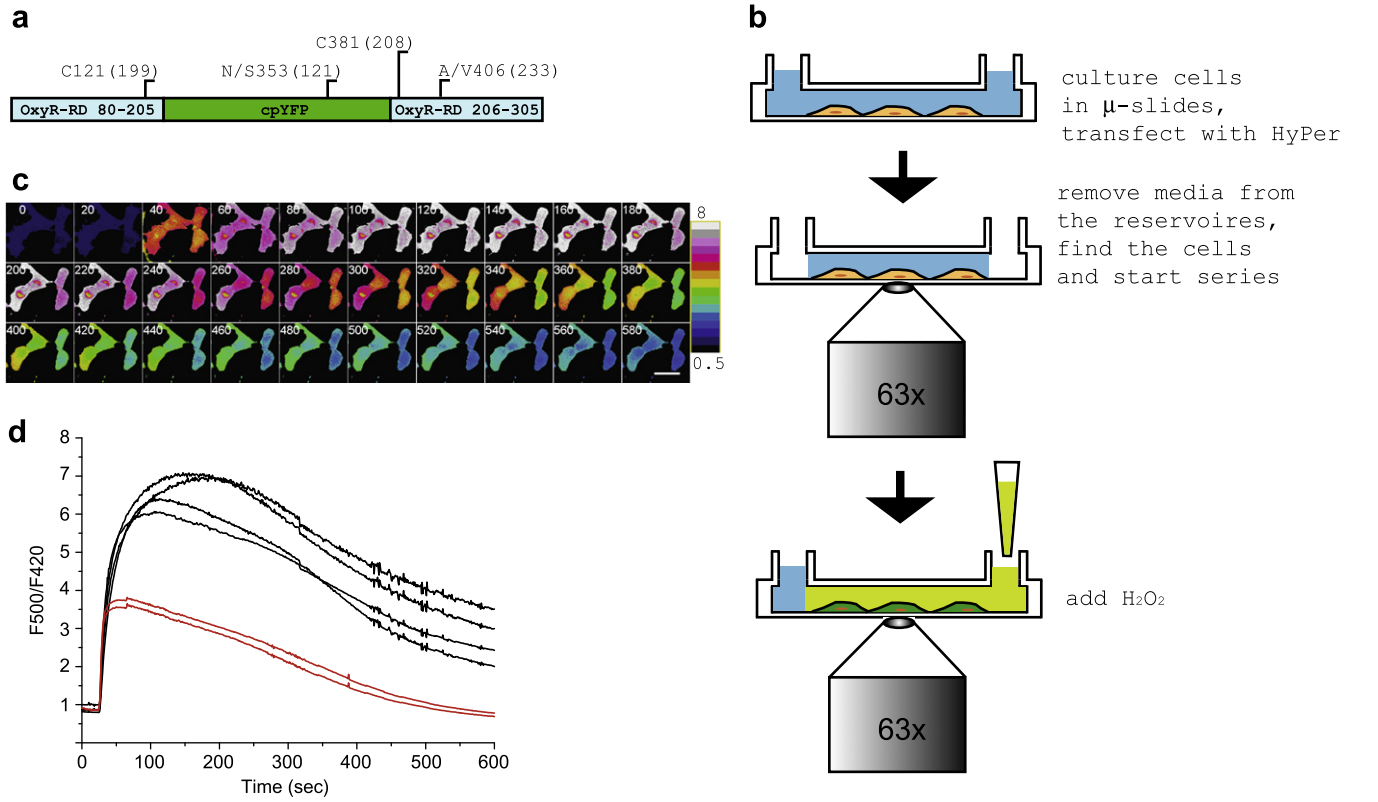

Figure 1. HyPer with N353S and A406V substitution demonstrates a high dynamic range in its ratio change upon addition of H_2O_2. (a) HyPer consists of cpYFP (green) inserted between residues 205 and 206 of OxyR-RD (blue). It contains two critical Cys residues, C121 and C381 (199 and 208 in wtOxyR). N353 corresponds to N121 in wtGFP. A406 is A233 in wtOxyR. (b) Scheme of the experiment with cells cultured and transfected in μ-slides. (c) Images of ratio F500/F420 change in cells transfected with HyPer-N353S-A406V exposed to 100 μM H_2O_2. Numbers indicate timing in seconds. H_2O_2 was added between the 2nd and 3rd frames shown. Scale bar 40 μm. (d) Timing of ratio change in cells shown on panel c (black lines) compared to HyPer expressing cells (red lines).

substitutions. Addition of C-terminal NES to HyPer without mutations had no effect on the dynamic range of the probe (data not shown). We therefore introduced each mutation separately into HyPer and expressed the resulting proteins in HeLa cells. Whereas the N353S substitution had no effect on HyPer's spectral properties, the A406V mutant appeared to exhibit an elevated dynamic range (Fig. 2a and b). The A406V substitution was therefore the sole cause of the property change. We named this probe HyPer-2.

We next compared the properties of intracellular HyPer-2 versus HyPer response to externally added H_2O_2. For this, we measured the half-oxidation and the half-reduction time of the probes. HyPer demonstrated faster oxidation and reduction than HyPer-2 (Fig. 2c and d). Both half-oxidation and half-reduction times of HyPer-2 were doubled compared to HyPer. This might indicate the reduced availability of the OxyR disulphide in HyPer-2 to reducing enzymes. It may also indicate increased sensitivity of HyPer-2 to H_2O_2 with higher probe-H_2O_2 reaction rates allowing a higher HyPer-2 oxidation rate in the presence of progressively decreasing concentrations of H_2O_2.

2.3. Oligomerization state of HyPer-2 versus HyPer

A233V mutation of OxyR corresponding to A406V in HyPer had been previously characterized as one destabilizing wtOxyR dimer interface.[8,12,13] We proposed that destabilization of the dimer interface leads to increased mobility of the 'redox loop', the region between a.a. 205 and 225 (wtOxyR nomenclature).[8] α-Helix hosting A233 is (i) packed into the dimer interface and (ii) flanks C-terminally the 'redox loop' into which the cpYFP is incorporated in HyPer. We performed gel-filtration chromatography to evaluate oligomerization states of HyPer and HyPer-2 (Fig. 3). Surprisingly, whereas HyPer appeared to be eluted as a mixture of dimers and monomers in concentrated samples or to be monomeric when diluted, HyPer-2 showed strong dimerization independently on the concentration of the protein. It suggests either that HyPer and HyPer-2 have a different structure of the interface compared to wtOxyR or that the substitution of A233 to the more hydrophobic Val stabilizes the HyPer interface via hydrophobic interaction with I110 and L124 (wtOxyR numbers).[8]

Notably, the ex497/ex420 ratio is higher for the dimers compared to the monomers (Fig. 3b). Therefore, it could be suggested that HyPer and HyPer-2 may change spectral properties upon dimerization. Our observations (unpublished data) show that ex497/ex420 ratio of reduced HyPer within the living cells resembles the ratio of the monomeric form of HyPer shown in Figure 3b suggesting HyPer exists in the monomeric form in the cell. Good performance of HyPer in fusions also supports its monomeric nature. However, for HyPer-2 the overall amplitude of its response to H_2O_2 may theoretically reflect two sequential processes, oxidation and oxidation-induced dimerization, which both may increase the ratio. This model could also explain slow response of HyPer-2 because its dimerization after oxidation may take time.

2.4. Detection of endogenous cellular H_2O_2 with HyPer-2

HyPer has been previously shown as a suitable probe for monitoring low amounts of H_2O_2 produced upon activation of growth factor receptors.[7,14,15] The dynamic range of HyPer-2 could be beneficial for signaling H_2O_2 studies because the oxidant is produced in subsaturating concentrations. We therefore stimulated NIH-3T3 fibroblasts expressing HyPer-2-NES or HyPer-Cyto with 10 ng/ml PDGF. All the cells responded by a progressive increase in H_2O_2 (Fig. 4). However, cells that express HyPer-2-NES demonstrated a higher amplitude of fluorescence response than those expressing regular HyPer. Therefore, HyPer-2 is more suitable for monitoring low concentrations of endogenous H_2O_2 than HyPer.

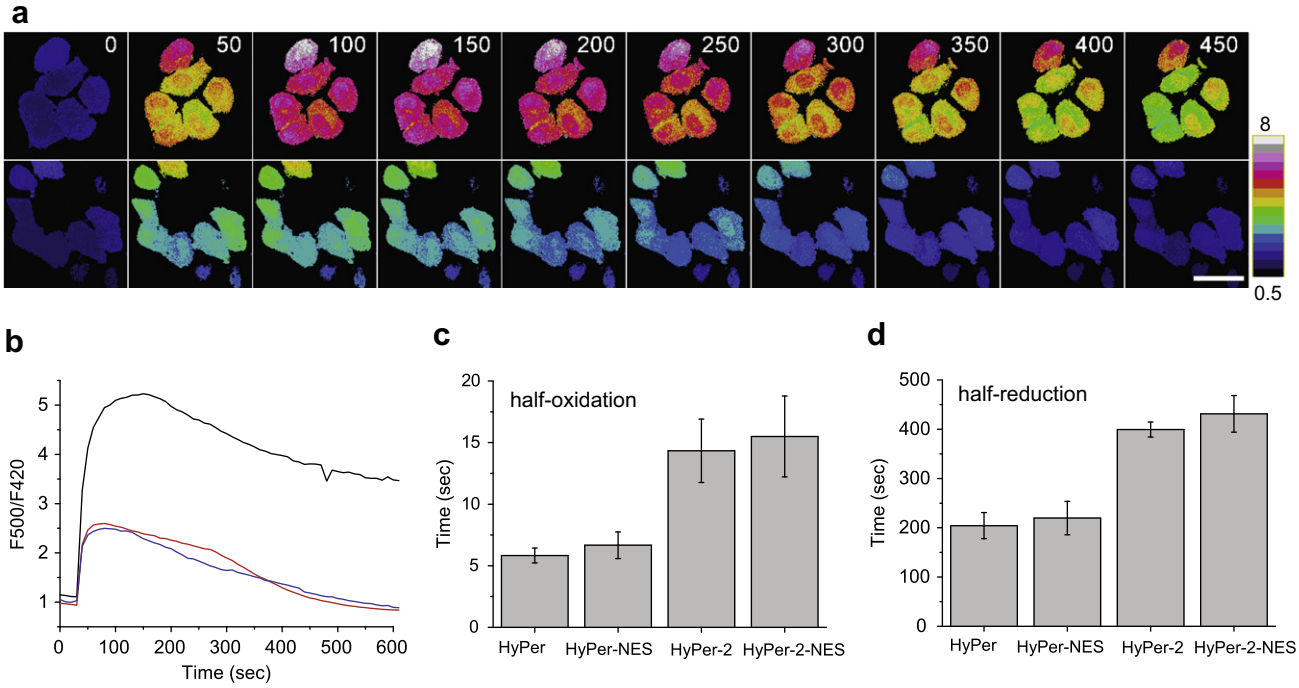

Figure 2. HyPer-2 versus HyPer response on H_2O_2. (a) Changes in ratio F500/F420 of HyPer-2 (upper raw) versus HyPer (lower raw). Numbers indicate time in seconds and show timing of both upper and lower rows. Scale bar 40 μm. (b) Typical profiles of the ratio F500/F420 change in individual cells expressing HyPer-2 (black line), HyPer-N353S (blue line) or HyPer (red line). (c) Time of half-oxidation of HyPer and HyPer-2 in cells upon addition of H_2O_2. Error bars indicate SEM values. (d) Time of half-reduction of HyPer and HyPer-2 in cells upon addition of H_2O_2. Zero time corresponds to the peak of the ratio. Error bars indicate SEM values. Data on (c) and (d) are the results of five independent experiments for HyPer, 6 for HyPer-2, 6 for HyPer-NES and 4 for HyPer-2-NES.

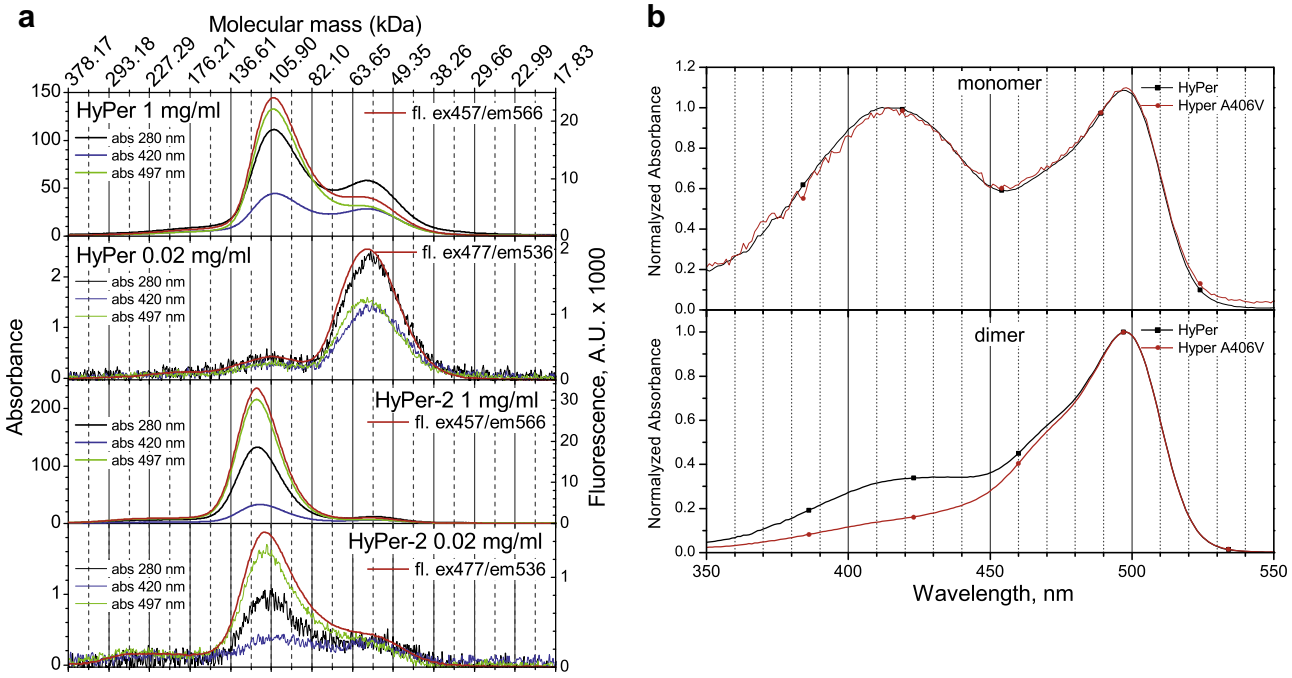

Figure 3. Gel-filtration elution profiles and excitation spectra of HyPer and HyPer-2. (a) Whereas HyPer (two upper plots) is eluted as a dynamic mixture of monomers and dimers, HyPer-2 (two lower plots) is a dimer independently on the protein concentration. (b) Excitation spectra of monomers and dimers of HyPer and HyPer-2.

3. Discussion

We introduced HyPer-2, the improved version of HyPer, a genetically encoded sensor for H_2O_2. The dynamic range of F500/F420 ratio change is 6, which is twice as high as in HyPer. This improvement was a result of a single point mutation changing Ala 406 for a Val residue. HyPer consists of two domains: a circularly permuted fluorescent protein (cpYFP) inserted into a regulatory domain of OxyR (OxyR-RD). The A406V substitution corresponds to A233V of wtOxyR. This mutation is one of several well-studied mutations of OxyR.[8,12,13] OxyR A233V is a constitutively active mutant probably due to reduced dimerization.[12,13] In case of full-length OxyR, activity means binding of OxyR to a specific DNA region and transcription from the corresponding promoter. Therefore OxyRA233V binds DNA irrespectively of the redox state of its dicysteine pair. Alanine 233 is one of the key residues of the interface between OxyR monomers in the dimer.[8] Substitution to the bigger Val residue has been shown to destabilize this interface resulting in a conformational shift in OxyR that improves DNA binding.[8,12,13] In case of HyPer, the same mutation led to the stabilization of the dimer interface leading to changes in mobility of the 'redox loop', the region flanked by position 205 (wtOxyR nomenclature) and a short alpha-helix participating in the dimer interface and containing the residue 233 (Fig. 5). cpYFP is inserted between a.a. 205 and 206. Therefore conformational changes in this region are critical for shifts in the cpYFP spectrum.

In our previous attempts to improve HyPer we mutated cpYFP and the linkers between the fluorescent protein and OxyR-RD. It seemed logically that the 'naturally designed' sensing part should be kept intact to preserve activity. Our results presented here show that the mutagenesis of this part is a promising strategy of the sensor improvement. In fact, this strategy was successfully used for the rational design of calcium probes. Tian and co-authors modified EF-hands in the Ca^{2+}-sensing domain to increase the affinity of the sensor to Ca^{2+} to produce GCaMP3.[16]

For most genetically encoded sensors, the limiting step in property improvement is the number of clones that can be manually screened. In case of simple fluorescent protein, any easy to detect parameter such as brightness or maturation speed can serve as a readout for mutagenesis. Fluorescent sensor candidates need to be visualized twice—before and after the change in the measured signal. The absence of high throughput strategies for sensor improvement restricts the potential applicability of the probes because most of the sensors published have a low dynamic range which prevents more general applications.

HyPer, and now HyPer-2, have been used to monitor the generation of H_2O_2 produced by cells activated by various growth factors, namely, NGF,[7] EGF,[14] PDGF, and insulin.[15] Detection of H_2O_2, therefore, can be used as readout in high throughput/high content screening of chemicals inhibiting RTK pathways and in the search for isoform-specific NADPH oxidases (Nox) inhibitors. HyPer or HyPer-2 need to be expressed in a proper cell line expressing the receptor of interest or a specific Nox isoform. Then, after addition of compounds and the agonist, cells expressing HyPer or HyPer-2 can be fixed with up to 4% paraformaldehyde and the HyPer emission ratio is acquired. Apart from the for above-mentioned receptors, many other growth factor and cytokines receptors and even some GPCRs that activate NADPH oxidases[4] may be assayed using HyPer/HyPer-2 in the future. We believe that HyPer-2 will be useful in novel screening platforms replacing the often used multistep screens based on phospho-MAPKs immunostaining.[17]

Final words should be said about influence of luck on experimental results. Three years of site-directed and random mutagenesis, screening of hundreds of clones in search for better mutant of HyPer did not give us an improved sensor. In fact, most variants performed worse then the original one. The first real improvement of the sensor properties came by chance as a side effect of the subcloning procedure. There is a phrase attributed to a famous biochemist Isaac Asimov: 'The most exciting phrase to hear in science, the one that heralds new discoveries, is not 'Eureka!' (I found it!) but 'That's funny . . .'

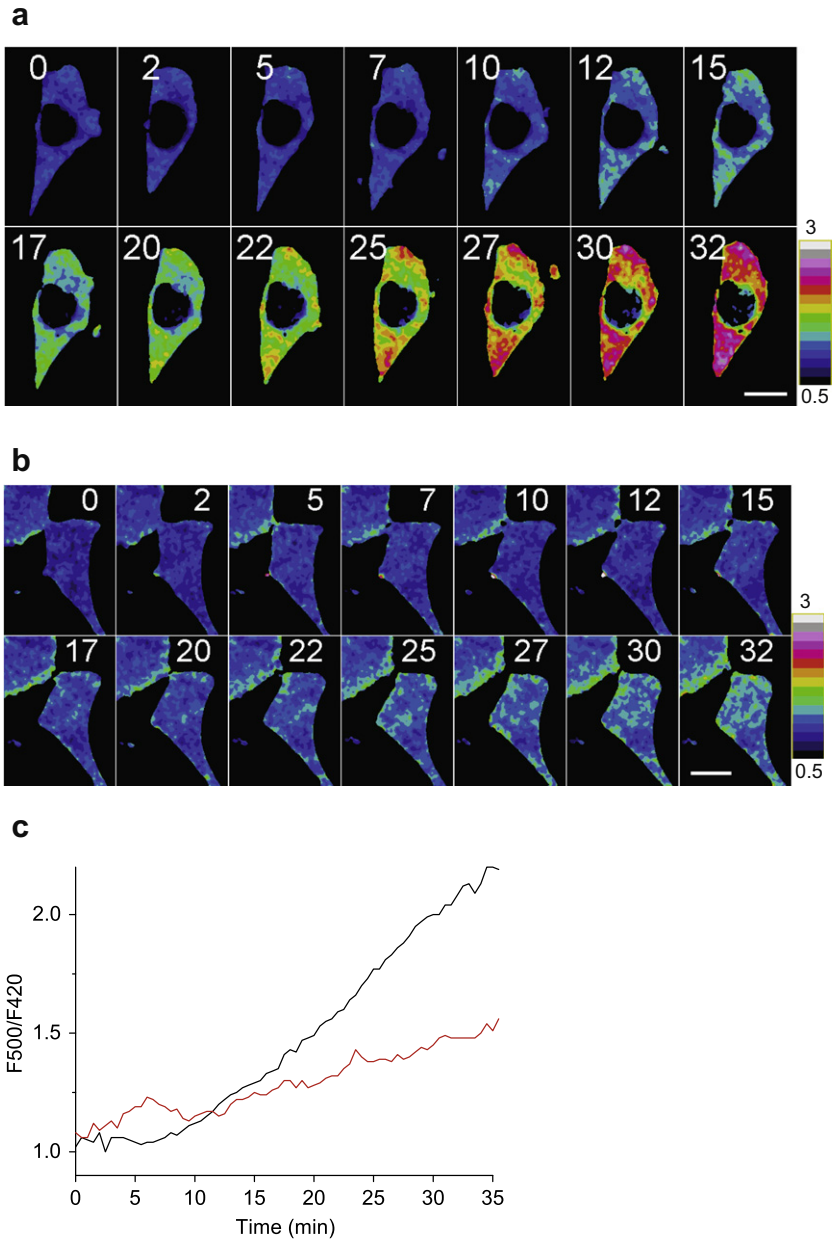

Figure 4. HyPer-2 versus HyPer response on H_2O_2 generated intracellularly upon addition of PDGF to NIH 3T3 cells. (a) Confocal images of a HyPer-2-NES expressing cell after stimulation with 10 ng/ml PDGF. Scale bar 20 μm. (b) Confocal images of a HyPer-Cyto expressing cell after stimulation with 10 ng/ml PDGF. Scale bar 20 μm. (c) Profiles of F500/F420 ratio change in the cells shown on the panel a (black line) or panel b (red line). PDGF is added at time zero.

4. Experiments

4.1. Materials

H_2O_2 and molecular weight markers for gel-filtration were from Sigma. Hanks balanced salts solution (HBSS) was from PanEko (Russia), DMEM, MEM, Opti-MEM, FCS and FuGene6 transfection reagent were from Invitrogen. μ-Slides-IV were from IBIDI, glass bottom dishes were from MatTec. HeLa and NIH-3T3 cells were from ATCC. HyPer expression vectors were from Evrogen.

4.2. Cell culture and transfection

HeLa-Kyoto and NIH-3T3 cells were cultured in DMEM supplemented with 10% FCS at 37 °C in atmosphere containing 95% air and 5% CO_2. Cells were splitted every 2nd day and seeded to the μ-slides-IV. After 12–24 h cells were transfected by the mixture of vector DNA and FuGene6 transfection reagent according to the liposomes manufacturer recommendations with the following optimization: because of a small volume of the μ-slide-IV, ready liposome-DNA solution was mixed with 10× volume of cell culture medium and used to replace the culture medium inside the channels of μ-slide-IV. Detailed protocols of media changing in μ-slides can be found at www.ibidi.com.

For experiments with growth factors, NIH-3T3 cells were seeded to glass bottom dishes. Twenty-four hours later cells were transfected by the mixture of vector DNA and FuGene6 transfection reagent according to the liposomes manufacturer recommendations.

4.3. Stimulation of the cells and imaging

Twenty-four hours after transfection the culture medium was changed to either HBSS (for experiments with externally added H_2O_2) or MEM without phenol red and serum (for PDGF stimula-

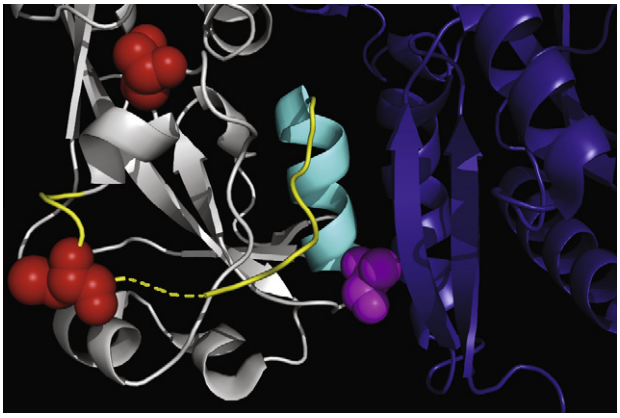

Figure 5. Image of the reduced OxyR-RD structure (PDB ID 1I69). C199 (upper) and C208 (lower) are shown in red. The flexible region of OxyR from a.a. 205 to 225 is yellow; the α-helix facing the dimer interface and hosting A233 (magenta) is shown in cyan. The second monomer of the dimer is dark blue. The image was obtained using PyMOL software.

tion). μ-Slides-IV with HeLa cells were transferred onto the microscopic stage of the widefield (Leica 6000) microscope equipped with an HCX PL APO lbd.BL 63x 1.4NA oil objective. FRET filter cube together with external CFP and YFP excitation filters were used to sequentially excite two excitation peaks of HyPer detecting emission using external YFP filter. Laser scanning confocal inverted microscopes Carl Zeiss LSM 510-META equipped with an HCX PL APO lbd.BL 63x 1.4NA oil objective and environmental chamber was used for growth factor stimulation experiments. Laser lines (405–488 nm) were used to sequentially excite two excitation peaks of HyPer detecting emission at 500–550 nm wavelength range. After 6 h (NIH-3T3) of incubation in serum-free medium, glass bottom dishes were transferred onto the microscopic stage. NIH-3T3 cells were stimulated by adding 10 ng/ml PDGF-BB. HeLa cells were stimulated by 100 μM H_2O_2.

4.4. Time series processing

Time series were analyzed using ImageJ free software downloaded from EMBL ALMF website (http://www.embl.de/almf/). Stacks of 420–500 nm (correspond to 2 HyPer excitation peaks) were Gaussian filtered with sigma radius 2 (skipped for widefield images) and background was subtracted. Images were converted to 32 bit and 420 nm stack was thresholded to remove pixel values from background (Not-a-Number function). Five hundred nanometers stack was divided to 420 nm stack frame-by-frame. The resulted stack was pseudocolored using 'Ratio' lookup table. Time course of HyPer fluorescence was calculated for regions of interest (ROIs) inside the imaged cell.

4.5. HyPer oligomerisation state estimation

Gel filtration chromatography was performed using a Superdex 200 10/300 GL column (Amersham Biosciences), equilibrated with 40 mM Tris–HCl (pH 7.5), 150 mM NaCl buffer at a flow rate of 0.4 ml/min. Elution profiles were monitored by absorbance at 280, 420, and 497 nm using a Varian ProStar 335 diode array detector and by fluorescence using in-line Varian ProStar 363 fluorescence detector. To obtain a fluorescence signal within a dynamic range of the detector, excitation/emission wavelengths were 457/566 nm for 1 mg/ml samples or 477/536 nm for 0.02 mg/ml samples. Apparent molecular masses were calculated by interpolating an elution volume versus log (molecular mass) calibration curve using ferritin (440 kDa), catalase (232 kDa), aldolase (158 kDa), BSA (67 kDa), ovalbumin (43 kDa), chymotrypsinogen A (25 kDa), and ribonuclease A (13.7 kDa).

Acknowledgments

The work is supported by Federal Education Agency (project no. P256), grant of the President of Russian Federation (MK-3567.2009.4), the Russian Academy of Sciences Program in Molecular and Cell Biology, the Russian Foundation for Basic Research (09-04-12235, 10-04-01561) and the Howard Hughes Medical Institute (55005618). K.N.M. received FEBS short-term fellowship.

Supplementary data

Supplementary data associated with this article can be found, in the online version, at doi:10.1016/j.bmc.2010.07.014. These data include MOL files and InChiKeys of the most important compounds described in this article.

References and notes

1. Droge, W. *Physiol. Rev.* **2002**, *82*, 47.
2. Winterbourn, C. C. *Nat. Chem. Biol.* **2008**, *4*, 278.
3. Rhee, S. G. *Science* **2006**, *312*, 1882.
4. Bedard, K.; Krause, K. H. *Physiol. Rev.* **2007**, *87*, 245.
5. Meng, T. C.; Fukada, T.; Tonks, N. K. *Mol. Cell.* **2002**, *9*, 387.
6. Lee, S. R.; Kwon, K. S.; Kim, S. R.; Rhee, S. G. *J. Biol. Chem.* **1998**, *273*, 15366.
7. Belousov, V. V.; Fradkov, A. F.; Lukyanov, K. A.; Staroverov, D. B.; Shakhbazov, K. S.; Terskikh, A. V.; Lukyanov, S. *Nat. Methods* **2006**, *3*, 281.
8. Choi, H.; Kim, S.; Mukhopadhyay, P.; Cho, S.; Woo, J.; Storz, G.; Ryu, S. *Cell* **2001**, *105*, 103.
9. Zheng, M.; Aslund, F.; Storz, G. *Science* **1998**, *279*, 1718.
10. Lee, C.; Lee, S. M.; Mukhopadhyay, P.; Kim, S. J.; Lee, S. C.; Ahn, W. S.; Yu, M. H.; Storz, G.; Ryu, S. E. *Nat. Struct. Mol. Biol.* **2004**, *11*, 1179.
11. Wang, X.; Mukhopadhyay, P.; Wood, M. J.; Outten, F. W.; Opdyke, J. A.; Storz, G. *J. Bacteriol.* **2006**, *188*, 8335.
12. Kullik, I.; Stevens, J.; Toledano, M. B.; Storz, G. *J. Bacteriol.* **1995**, *177*, 1285.
13. Kullik, I.; Toledano, M. B.; Tartaglia, L. A.; Storz, G. *J. Bacteriol.* **1995**, *177*, 1275.
14. Markvicheva, K. N.; Bogdanova, E. A.; Staroverov, D. B.; Lukyanov, S.; Belousov, V. V. *Methods Mol. Biol.* **2009**, *476*, 76.
15. Espinosa, A.; Garcia, A.; Hartel, S.; Hidalgo, C.; Jaimovich, E. *J. Biol. Chem.* **2009**, *284*, 2568.
16. Tian, L.; Hires, S. A.; Mao, T.; Huber, D.; Chiappe, M. E.; Chalasani, S. H.; Petreanu, L.; Akerboom, J.; McKinney, S. A.; Schreiter, E. R.; Bargmann, C. I.; Jayaraman, V.; Svoboda, K.; Looger, L. L. *Nat. Methods* **2009**, *6*, 875.
17. Olive, D. M. *Expert Rev. Proteomics* **2004**, *1*, 327.